Natural images and contrast encoding in bipolar cells in the retina of the land- and aquatic-phase tiger salamander

DWIGHT A. BURKHARDT, PATRICK K. FAHEY, AND MICHAEL A. SIKORA
Departments of Psychology and Graduate Program of Neuroscience, University of Minnesota, Minneapolis, Minnesota

Abstract

Intracellular recordings were obtained from 57 cone-driven bipolar cells in the light-adapted retina of the *land-phase* (adult) tiger salamander (*Ambystoma tigrinum*). Responses to flashes of negative and positive contrast for centered spots of optimum spatial dimensions were analyzed as a function of contrast magnitude. On average, the contrast/response curves of depolarizing and hyperpolarizing bipolar cells in the *land-phase* animals were remarkably similar to those of *aquatic-phase* animals. Thus, the primary retinal mechanisms mediating contrast coding in the outer retina are conserved as the salamander evolves from the aquatic to the land phase. To evaluate contrast encoding in the context of natural environments, the distribution of contrasts in natural images was measured for 65 scenes. The results, in general agreement with other reports, show that the vast majority of contrasts in nature are very small. The efficient coding hypothesis of Laughlin was examined by comparing the average contrast/response curves of bipolar cells with the cumulative probability distribution of contrasts in natural images. Efficient coding was found at 20 cd/m^2 but at lower levels of light adaptation, the contrast/response curves were much too shallow. Further experiments show that two fundamental physiological factors—light adaptation and the nonlinear transfer across the cone-bipolar synapse are essential for the emergence of efficient contrast coding. For both land- and aquatic-based animals, the extent and symmetry of the dynamic range of the contrast/response curves of both classes of bipolar cells varied greatly from cell to cell. This apparent substrate for distributed encoding is established at the bipolar cell level, since it is not found in cones. As a result, the dynamic range of the bipolar cell population brackets the distribution of contrasts found in natural images.

Keywords: Retinal bipolar cells, Contrast encoding, Natural images, Land-phase tiger salamander, Horizontal cells, Retina

Introduction

In all vertebrate retinas, bipolar cells serve as the primary inter-neurons between photoreceptors and the ganglion cells, the retinal output neurons. It is now well established from intracellular recordings that bipolar cells impart major transformations on the signals they receive from the photoreceptors (Werblin & Dowling, 1968; Burkhardt & Fahey, 1998; DeVries, 2000; Dacey et al., 2000; Rieke, 2001; Thoreson & Burkhardt, 2003; Wu, 2003; Burkhardt et al., 2004; Copenhagen, 2004; Nelson & Kolb, 2004; Sterling, 2004). The ultimate function of retinal neurons, and sensory neurons in general, is to efficiently encode the information in the natural environment (Simoncelli & Olshausen, 2001; Sterling, 2004). Most objects in the visual world are detected on the basis of luminance contrast, the difference between the intensity of objects and their backgrounds.

With the goal of gaining further insight into the natural function of retinal bipolar cells, we have made measurements of the luminance contrast in 65 natural scenes using a spatial sampling procedure with dimensions similar to those of bipolar cell receptive fields. Our results, which agree reasonably well with several past reports based on *different* sampling procedures and sites, support the essential conclusion that, in nature, low contrasts are very common while extremely high contrasts are rare. Thus, if contrast encoding were optimal, bipolar cells should show high gain to low contrasts and saturating responses for high contrasts. When the retina is well light adapted, we show that bipolar cells in the *land-phase* tiger salamander conform well with these general expectations. In particular, the *average* contrast/response curves of both classes of bipolar cells approximate the cumulative probability distribution of the contrasts in natural images. This correspondence provides evidence for the efficient coding principle first proposed and demonstrated in the invertebrate visual system by Laughlin (1981, 1987). The present report is the first to show that,

---

Address correspondence and reprint requests to: Dwight A. Burkhardt, University of Minnesota, Department of Psychology, 75 E. River Road, 218 Elliott Hall, Minneapolis, MN 55455, USA. E-mail: burkh001@tc.umn.edu

in the vertebrate retina, this encoding strategy is largely established distally, in the bipolar cells.

Since the contrasts of objects in nature are invariant with the intensity of the incident light, ideally, efficient coding should hold over all ambient light intensities. To the contrary, we will show that efficient coding in cone-driven bipolar cells is not achieved when the background light is low. This finding and further experiments in both land- and aquatic-phase tiger salamanders show that two physiological factors, the level of light adaptation and nonlinear signal transfer across the cone-bipolar synapse, are critical for the emergence of efficient contrast encoding. From this perspective, our results provide a new rationale for the function of light adaptation and nonlinear signal transmission across the cone-bipolar synapse in vertebrate vision.

To adequately understand the basis of contrast encoding, the variance within the neuronal population may be as important as the *average* response of the population. Here we have been able to evaluate this issue from a sample of nearly 200 bipolar cells. In this analysis, we find striking variance in both the magnitude and symmetry of the dynamic range of the contrast response. From these measurements, we will show that the distribution of the dynamic range across the bipolar population brackets the distribution of contrasts found in the natural images and suggest that this could have been the driving evolutionary force for the emergence of distributed encoding by retinal bipolar cells.

This report is apparently the first to describe the response of neurons in the retina of the land-phase tiger salamander. Although the aquatic-phase tiger salamander (also called larval, juvenile, or neotenous) undergoes striking changes in physiology and morphology when it migrates from water to land (Pough et al., 2001; Zug et al., 2001), we provide evidence that the response of retinal neurons remains functionally stable. This result has implications for past research on aquatic-phase animals and the question of whether there is a need for retinal reorganization when the animal migrates from an aquatic to a terrestrial optical environment.

Materials and methods

Preparation, recording, and light stimulation

Intracellular recordings were made from superfused eyecup preparations of the tiger salamander (*Ambystoma tigrinum*), as previously described in detail (Burkhardt & Fahey, 1998; Fahey & Burkhardt, 2001; Burkhardt et al., 2004). Land-phase salamanders were obtained from Kons Scientific (Germantown, WI). Aquatic-phase animals were obtained from Kons Scientific and Charles Sullivan Co. (Nashville, TN). Measurements of contrast processing in aquatic-phase animals obtained from Kons or Sullivan did not differ appreciably although there may be some differences in other properties (Hare & Owen, 1995). The retina was superfused at about 1 ml/min with a Ringer solution composed of the following (in mM): 111 NaCl, 22 NaHCO$_3$, 2.5 KCl, 1.5 MgCl$_2$, 1.5 CaCl$_2$, and 9 dextrose. Intracellular recordings were made with glass micropippets which were filled with 0.25 M KAcetate and had resistances of 500–900 MΩ. Cell types were identified on the basis of functional criteria established in past work in the tiger salamander (Hare & Owen, 1990; Yang & Wu, 1991; Burkhardt & Fahey, 1998; Fahey & Burkhardt, 2001; Burkhardt et al., 2004). In brief, recordings assigned to bipolar cells had small receptive-field centers, typically giving their largest response to stimuli of about 250 μm in diameter. Stimuli of large diameter evoked smaller responses. In all cases, an annulus evoked a response of opposite

polarity to that evoked by central illumination. The present report deals exclusively with contrast responses under background illumination that isolates cone-driven bipolar cells (Burkhardt & Fahey, 1998). Normalized responses are analyzed exclusively in this report since no obvious relations were seen between the functional response properties of interest and absolute response amplitudes. The average total response amplitudes for our sample of land-phase animals were 17.7 mV ($n = 27$, ±4.05 S.D.) for depolarizing (Bd) cells and 15.2 mV ($n = 30$, ±2.8 S.D.) for hyperpolarizing (Bh) cells.

Responses to contrast steps of 0.5-s duration were generated by an active-matrix Liquid Crystal Display (Magnabyte m2x, Telex Communications, Minneapolis, MN) under computer control as previously described in detail (Burkhardt et al., 1998; Fahey & Burkhardt, 2001). The retina was held in a steady state of light adaptation by a background field of 20 cd/m^2. After penetrating a bipolar cell, the center of the receptive field was determined by flashing a 100 × 2000 μm slit at various positions on the retina. The diameter of a centered spot was then varied to find the optimal diameter for stimulating the central receptive-field mechanism. The optimum diameter ranged from about 100–500 μm, depending on the bipolar cell. On average, the optimum diameter was about 250 μm for aquatic animals and 210 μm for land animals but there was much overlap and these differences were not statistically significant. For horizontal cells, the stimulus was centered in the receptive field and set at 2200 μm thereby illuminating the entire receptive field.

In this report, contrast is specified as the logarithm of the contrast ratio: Contrast = $\log_{10}$ (F/B), where B is the steady background intensity and F is the light intensity prevailing during the flash. In this metric, contrast steps that increase or decrease the prevailing light by the same factor differ only in sign: for example, 10× increases and 10× decreases from the background are specified as contrasts of +1.0 and −1.0, respectively. The rationale for this contrast metric and its relation to the classic Weber contrast ($\Delta I/I$) is discussed in detail in (Fahey & Burkhardt, 2001). The bipolar cell response amplitude was measured from the baseline to the peak of the response evoked by the onset of the contrast step. As in the original analysis of Laughlin (Laughlin, 1981, 1987), the response amplitude was then normalized with the maximum amplitude to negative contrast set at 0.0 and the maximum response to positive contrast set at 1.0. When normalized in this way, the contrast/response curves for both hyperpolarizing and depolarizing bipolar cells range from 0 to +1.0. The present report deals exclusively with the peak response evoked by the contrast step, either negative or positive. Other possible measurements based on the sustained amplitude, the integrated voltage, or the off response have not been analyzed in detail and fall beyond the scope of the present report.

Measurement of contrast distributions of natural scenes

Digital photographs of 65 natural scenes were taken near the banks of Lake Nokomis and the Mississippi River in Minneapolis with a Nikon Coolpix 995 digital camera set in the black-and-white mode. The camera detector sensitivity was held constant at ISO400. The shutter speed and aperture were allowed to vary. The field of view was 47.9 × 35.9 deg. A broadband filter centered at 600 nm with a halfband pass of 80 nm (Edmund Scientific F-565-505) was placed in front of the camera lens to approximate the spectral sensitivity of the 610-nm cones, the predominant class of cones of the salamander retina. To emphasize scenes with a greater range

and larger number and of contrasts, large expanses of sky or water were avoided. All images were obtained on bright, cloudless days. Many of the scenes were selected to contain local areas of dark shadows and thus relatively high contrasts around their edges. Some images did not have borders between the sky and ground which may have introduced some bias against positive contrast. However, such an effect would appear to be quite minor to judge from an analysis of images with and without such borders.

Every image was calibrated by taking the picture twice—with and without a gray-scale calibration panel in the scene. The panel, which was precisely calibrated in the laboratory with a reflectometer, contained five segments with reflectances of 2.3, 7.6, 15, 54, and 90%, respectively. The image of the panel was viewed in Adobe Photoshop and the average digital value of each segment was measured. These measurements were used to construct a calibration curve for each image and thereby compute the relative intensity of all pixels in the image. The raw images were 2048 $\times$ 1536 pixels. Image processing was done in MATLAB. The spatial resolution was reduced by a factor of 10 for computational efficiency. A composite square, consisting of nine smaller squares was successively centered on each pixel location in the reduced image. At each pixel location, the average intensity of the central square and the average intensity of the eight surrounding squares were determined. The contrast was then computed as the logarithm of the contrast ratio: Contrast = $\log_{10} (C/S8)$, where C and $S8$ are, respectively, the average intensity of the central square and the average intensity of the eight surrounding squares. A histogram of the distribution of contrasts in the scene was constructed using a bin width of 0.05 contrast unit. The $\log_{10}$ metric for specifying contrast has been used extensively in past work because it has particular merit for analyzing negative and well as positive contrast. This point and conversion factors relative to two other contrast metrics, Michelson contrast and Weber contrast, are discussed in detail elsewhere (Fahey & Burkhardt, 2001).

The analysis described above was performed for four different spatial samples in which the central square subtended 1.9, 2.9, 4.8, and 9.6 deg. These angles correspond, respectively, to approximately 100, 150, 250, and 500 μm on the salamander retina. They were selected to span the range of receptive-field centers of bipolar cells found experimentally (Burkhardt & Fahey, 1998; Fahey & Burkhardt, 2001, 2003). Of these, a diameter of about 250 μm is most representative so primary emphasis in the Results section is given to the 4.8-deg sample.

For a small sample of images, the effect of basing the surround on the average of all surrounding pixels in the entire image was investigated while keeping the center at 4.8 or 1.9 deg. This procedure produced a modest broadening of the contrast distribution but was not pursued further since the focus of this report is to analyze contrast for spatial parameters that are relevant to the dimensions of both the surround and center of the receptive field of bipolar cells. For a small sample of images, the distribution of spatial frequency of the entire image was analyzed using MATLAB. When plotted in log–log coordinates, the magnitude plots were approximately linear with negative slope, in general agreement with many previous reports (Ruderman & Bialek, 1994; Simoncelli & Olshausen, 2001; Balboa & Grzywacz, 2003). However, the differences from image to image were relatively subtle and not subjected to further analysis.

Contrast distributions were also computed for a sample of 27 natural images taken from the data set of Dr. J.H. van Hateren (image numbers 16, 53, 129, 226, 264, 265, 311, 317, 327, 382, 389, 403, 406, 477, 478, 535, 538, 650, 693, 1015, 1025, 1131,

1184, 3415, 3501, 3350, and 3537). These and all images in his extensive set may be viewed at http://hlab.phys.rug.nl/. We also analyzed contrast distributions for a sample of 25 underwater images (Balboa & Grzywacz, 2003). To our knowledge, these are the only *calibrated* measurements of underwater images reported to date. We are greatly indebted for Dr. Balboa for providing the original raw data from this study. The calibrated data of the van Hateren and the Balboa and Grzywacz data sets were analyzed with the identical procedure as described above for our image sample. Thus, the data from all these studies could be compared and summarized as histograms in units of $\log_{10}$ of the contrast ratio, as defined above.

Results

Contrast responses in the outer retina of land-phase animals

As a first step toward analyzing the contrast encoding in the outer retina of land-phase animals, the responses of the electroretinogram (ERG) and horizontal cells to full-field illumination (2-mm diameter) were studied. The traces in the top row of Fig. 1 show the ERG evoked by steps of positive contrast (left) and negative contrast (right), ranging from low contrasts of 0.15 to very high contrasts of 2.0 (see Fig. 1 legend). Although the amplitude of the ERG was small due to shunting in the superfused preparation, the signal/noise ratio was quite satisfactory for measuring the contrast response. The on-response to positive contrast steps is almost entirely due to the *b*-wave while a very small *a*-wave is detectable at very high contrast steps (+1.0 and +2.0). The on-response to negative contrast is the same polarity as that of the *b*-wave, as expected if it is largely due to the ERG *d*-wave. The insert at the top of Fig. 1 shows the contrast/response curve for measurements of peak-to-trough amplitude of the on-response for this representative recording. The maximum response to positive contrast is larger than that due to negative contrast. Hence, the ERG is "positive contrast dominant". The response amplitudes to low contrasts of both polarities are quite small. Thus, the contrast gain is low. The low contrast gain is also apparent in Fig. 1 since the responses to 0.15 contrasts (arrows) are only about 1/5–1/6 of the responses evoked by maximum contrast. Overall, the features of the contrast/response curves of the ERG of land-phase animals shown in Fig. 1 were similar to those found previously for aquatic-phase animals. This provides evidence that mechanisms in the outer retina are relatively similar in land and aquatic-phase animals.

The lower traces in Fig. 1 show representative contrast responses for a horizontal cell. The response polarity depends on the contrast polarity. The amplitude was measured from the baseline to the peak of the response evoked by the onset of the contrast step. The insert shows the contrast/response for this recording, which is representative of our sample of 16 horizontal cells in land-phase animals. The curve shows evidence for positive contrast dominance and relatively small responses for low contrasts, that is, low contrast gain. Thus, like the ERG, the responses to $\pm$0.15 contrasts (arrows) are a small fraction of the maximum responses. Overall, the quantitative properties of the contrast/response of horizontal cells of land-phase animals were quite similar to those found previously for aquatic-phase animal at the same level of light adaptation, 20 cd/m^2 (Fahey & Burkhardt, 2001). In both, the contrast gain is low and the dynamic range is large.

Fig. 2 shows responses to steps of positive contrast (left) and negative contrast (right) for a depolarizing bipolar cell (Bd) and a
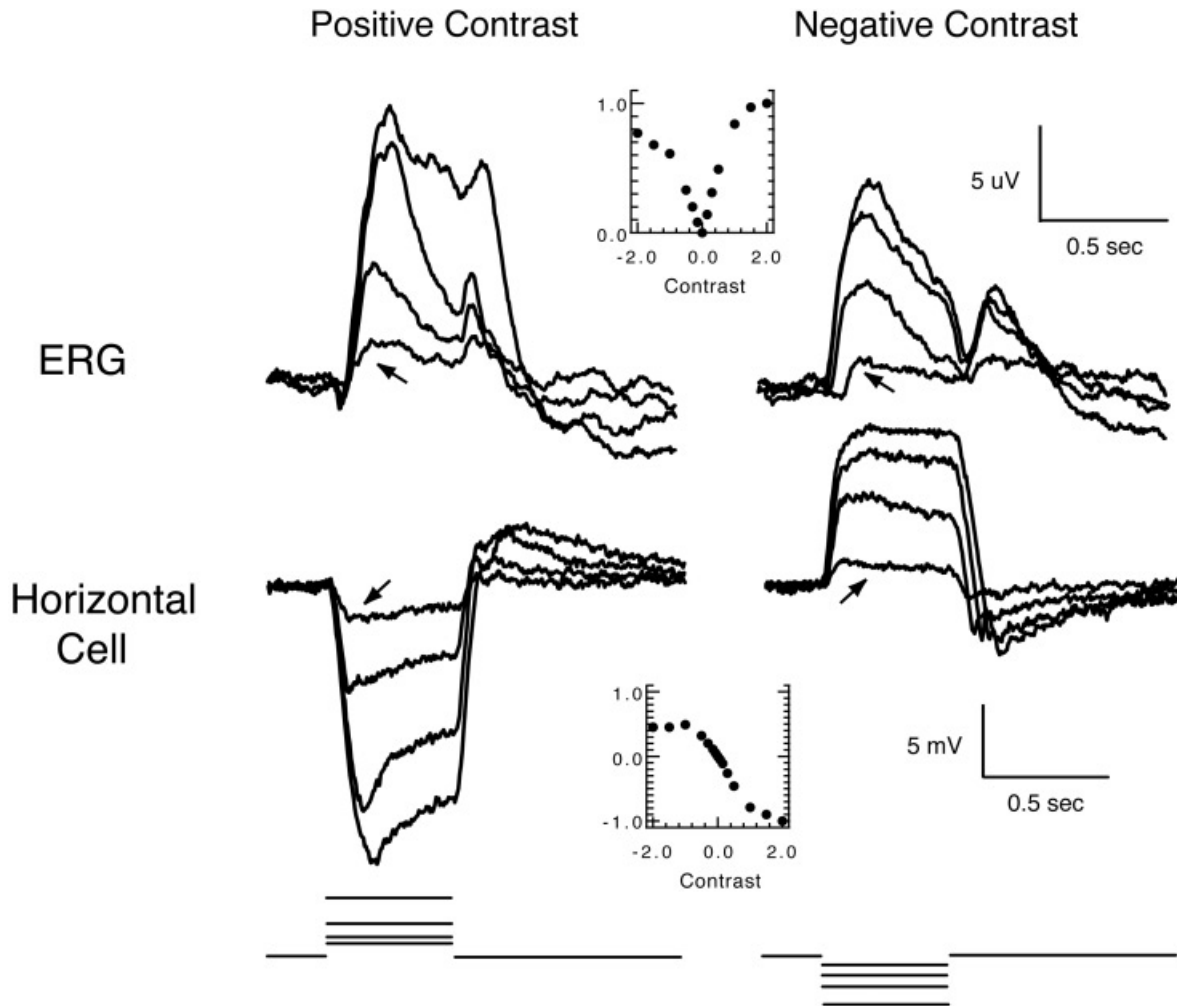
Fig. 1. Responses to contrast steps for the electroretinogram and a horizontal cell in the land-phase tiger salamander. The contrast steps are in an ascending series of 0.15, 0.50, 1.0, and 2.0 contrast for both negative and positive contrast. The arrows point to responses evoked by 0.15 contrast steps. The inserts show the measured contrast/response curves (see text).
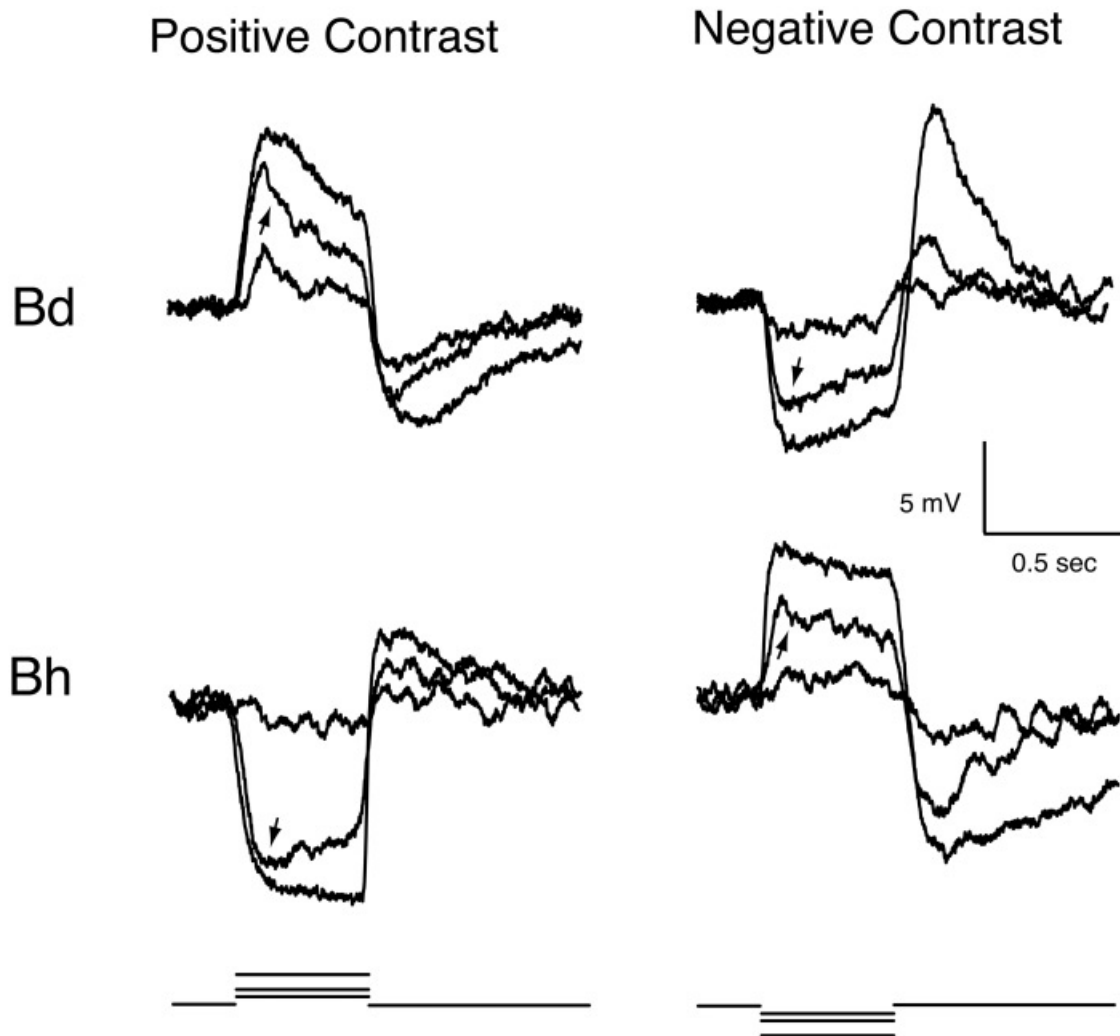
hyperpolarizing bipolar cell (Bh). As for horizontal cells and the ERG in Fig. 1, the retina was light adapted to a steady background illumination 20 cd/m². The contrast steps were spots of optimal diameter restricted to the center of the receptive field (see Methods). Both cells in Fig. 2 give clear responses to very small contrasts (± 0.03) and very substantial responses to contrasts of ± 0.15 (arrows). The responses are virtually saturated at contrasts of ± 1.0. In sum, from Figs. 1 and 2 it is clear that the contrast encoding by bipolar cells differs markedly from that of horizontal cells and the electroretinogram.

Contrasts in natural images

To more fully evaluate the quantitative characteristics and functional significance of the contrast response of bipolar cells in land-phase animals, it is instructive to evaluate the contrasts found in natural environments. In this section, we summarize our measurements of contrasts in a sample of natural images and then compare our results with previous reports that used different sampling and/or analytic procedures. As elaborated in Methods, our analysis is based on a sample of 65 calibrated images of natural

terrestrial scenes. Fig. 3 shows examples of six images in our sample, chosen to represent the range of the scenes analyzed. Fig. 4 shows the corresponding contrast histograms for these images. The central reference square was 4.8 deg, the typical extent of the central region of the receptive field of bipolar cells (see Methods). Fig. 4 shows that the details of the contrast distributions can vary considerably across scenes. The distributions range from narrow (*B*) to wide (*F*) and show varying degrees of asymmetry around zero contrast. We will treat the issue of the variance of the contrast distributions in more detail later, after first analyzing the prominent features of average distributions found in the present and previous reports.

The average histogram for all 65 images for the case of the 4.8-deg center reference is shown in the middle histogram of Fig. 5. It is clear that the vast majority of contrasts were quite low, since the distribution peaks near zero contrast and then falls rapidly for both positive and negative contrasts. The distribution is not perfectly symmetrical, being slightly skewed in favor of negative contrast. Similar results were found when the images were analyzed either with a 1.9-deg center reference (left histogram) or a 9.6-deg center reference (right histogram). As the area

Positive Contrast

Negative Contrast

Bd

Bh

5 mV

0.5 sec

Fig. 2. Responses to contrast steps for a depolarizing bipolar cell (top row) and a hyperpolarizing bipolar cell (bottom row) in the land-phase tiger salamander. Stimuli were spots centered in the receptive field and of optimal diameter for each cell: 99 μm (top) and 241 μm (bottom). The contrast steps are in an ascending series of 0.03, 0.15, and 1.0 for both negative and positive contrast. The arrows point to responses evoked by 0.15 contrast steps.

of the center reference is increased over a factor of about 25× in Fig. 5, the distributions broaden somewhat. Such broadening with increasing reference area was often seen when analyzing individual images but not invariably. Thus, depending on specific features of the individual scenes, the shape of the distribution could vary in other ways as a function of the size of the center reference area. Nevertheless, when averaged over a large number of images, the differences of the average histograms in Fig. 5 are modest. Hence, these results seem broadly consistent with the principle of spatial scale invariance in the contrast distributions of natural images suggested by the work of others (Ruderman & Bialek, 1994; Vu et al., 1997; Tadmor & Tolhurst, 2000). On the other hand, as will be documented later, the distribution broadened appreciably when the central reference square was made very small to subtend 0.2 deg.

Fig. 6 shows average contrast distributions based on image measurements of four other data sets. All data have been computed or transformed to the $\log_{10}$ contrast metric to provide a uniform basis for comparison. Figs. 6A and 6B, respectively, are based on

the reports of Laughlin (1981; Fig. 2) and Vu et al. (1997; their Fig. 6C). Their spatial sampling procedures differed considerably from ours. Laughlin measured the contrast between the mean intensity in a 50-deg surrounding area relative to the intensity in a 0.07-deg area convolved with a Gaussian spread function of 1.4-deg half-width. Vu et al. measured the intensity in 2-deg areas in 15-deg intervals across the scene and calculated the contrast between the intensity in each 2-deg reference area relative to the mean intensity of measurements on either side of the reference area.

Figs. 6C and 6D, respectively, show the results of applying our computational protocol with a 4.8-deg center area to 27 images taken from the data sets of J.H. van Hateren (http://hlab.phys. rug.nl/) and 25 images of Balboa and Grzywacz (Balboa & Grzywacz, 2003; R.M. Balboa, personal communication). Figs. 6A–6C, which are all based on samples from natural environments on land, are in reasonably good agreement with our measurements of Fig. 5. On the other hand, Fig. 6D is based on underwater images and somewhat narrower than those of the land scenes. All the
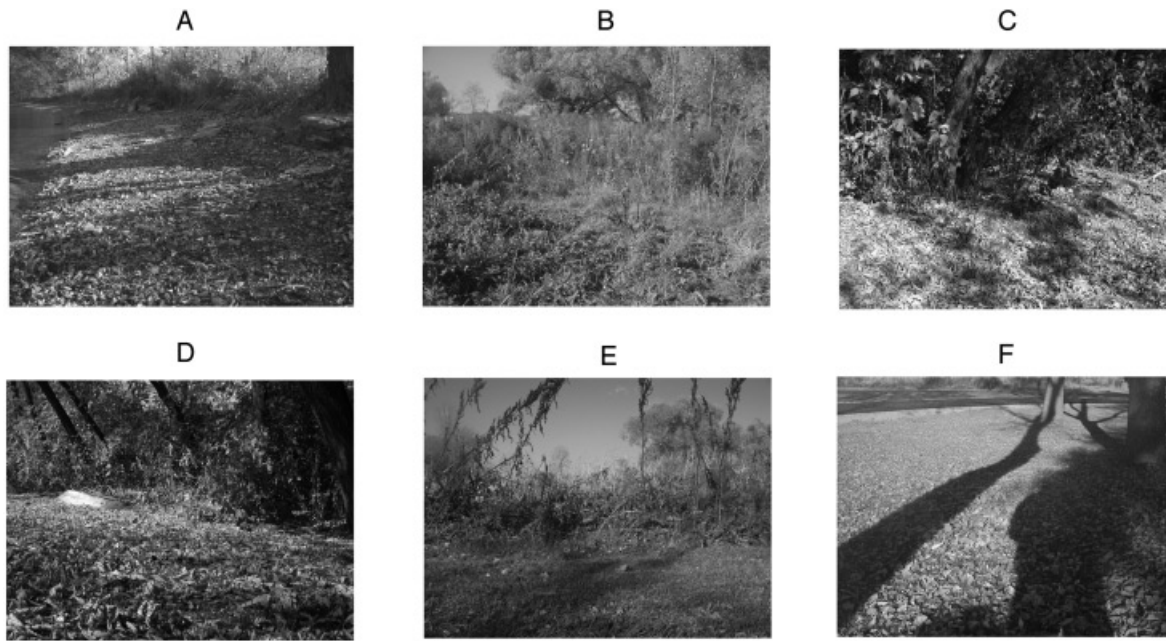
Fig. 3. Six scenes from the set of 65 natural images selected to represent the range of scenes in the image set.

distributions in Figs. 5 and 6 are sharply peaked and are neither Gaussian nor perfectly symmetrical. To compare these distributions quantitatively, we have measured the contrasts at which the distributions fall to the 50, 10, and 5% levels for both negative and positive contrasts. Table 1 summarizes the results for ten cases, including all those shown in Figs. 5 and 6. The contrast levels and their polarity are shown in the notation along the top. Contrast, as in the body of the table, is given in units of $\log_{10}$ contrast $\times$ 100 (see Table legend for further details). The top eight rows are for image samples in land environments and are remarkably similar
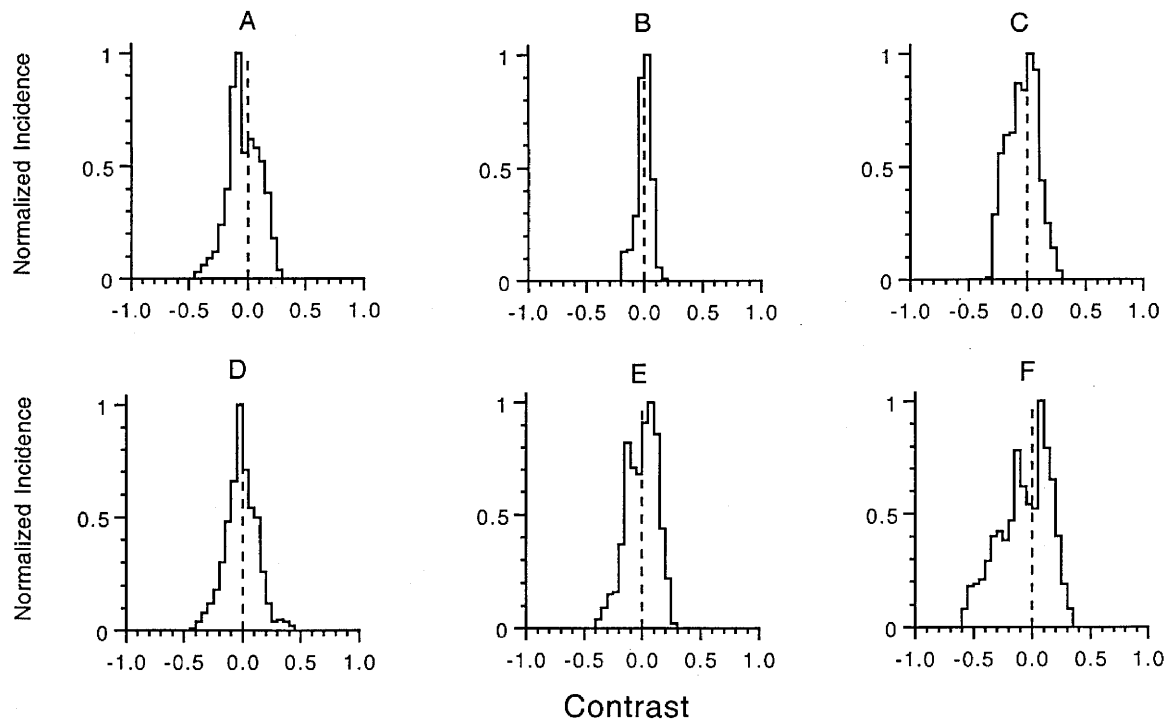

Fig. 4. Contrast histograms for the scenes of Fig. 3. The bin width is 0.05 contrast unit (see Methods for definition of contrast). In this figure and in Figs. 4 and 5, a dashed vertical line is inserted at zero contrast.
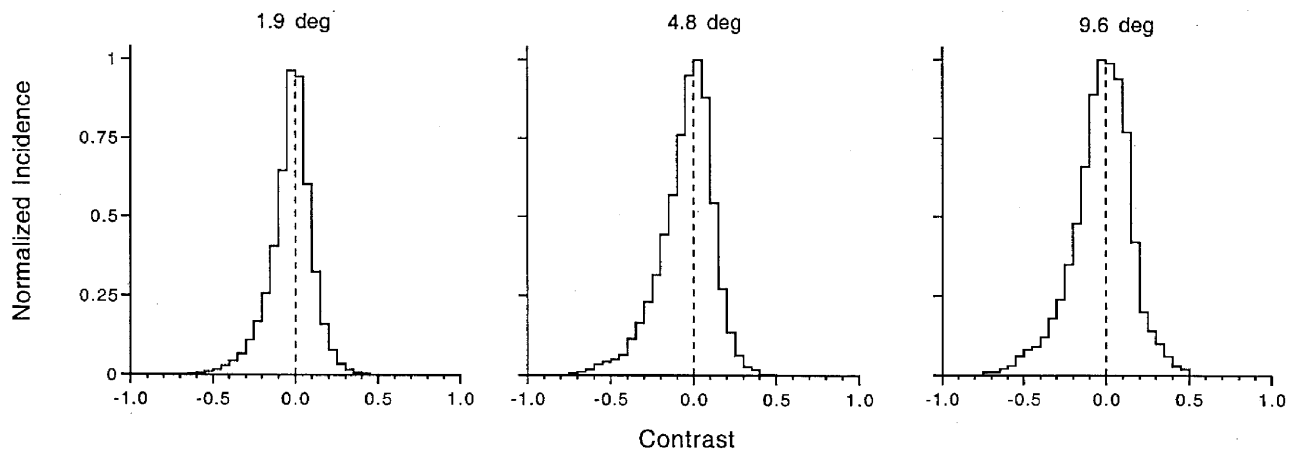
Fig. 5. Average contrast histograms for 65 images analyzed with respect to a central reference area of either 1.9, 4.8, or 9.6 deg.

across studies and sampling procedures, with the exception of the case for a very small (0.2-deg) reference center. The bottom two rows show measurements for underwater images Balboa and Grzywacz (Balboa & Grzywacz, 2003; R.M. Balboa, personal communication). The values are all smaller than that of the land distributions and the differences are larger for the large negative contrasts. Thus, on average, the contrast distributions are somewhat narrower underwater than on land.

Comparison of the contrast/response of bipolar cells and natural image distributions

The open circles and open triangles in Fig. 7 show, respectively, the average contrast response curves for depolaraizing (Bd) and

hyperpolarizing (Bh) bipolar cells for the land-phase salamander when the retina was light adapted to 20 cd/m^2. The response amplitude has been normalized as in the original analysis of Laughlin (1981) as described in detail in Methods. The line shows the cumulative probability of the contrast distribution obtained from our sample of natural images for the center size of 4.8 deg (Fig. 5, middle). The filled circles and crosses in Fig. 7 show, respectively, the average contrast/response curves for 63 Bd and 72 Bh cells collected from our past work on aquatic-phase animals on a background illumination of 20 cd/m^2 (Fahey & Burkhardt, 2001). The average contrast/response curves of Bd and Bh cells of the aquatic-phase animals are very similar to those of the land-phase animals. In both forms, the average contrast/response curves approximate the average cumulative contrast dis-
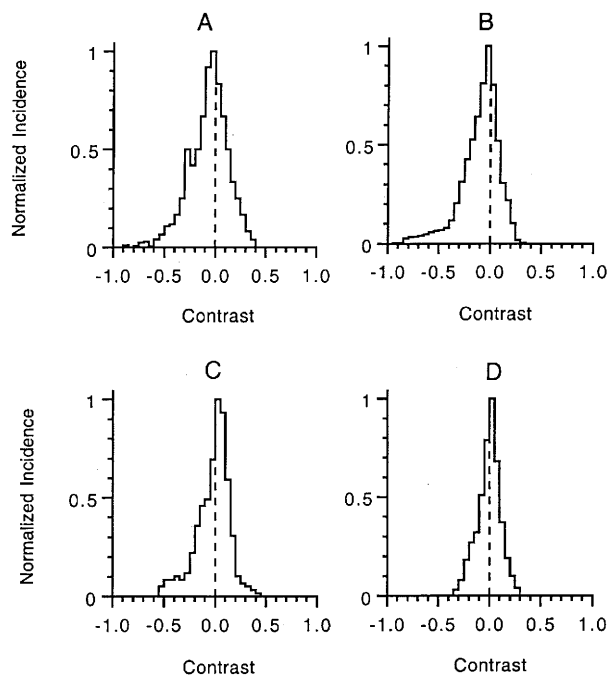

Fig. 6. Average contrast histograms computed from image samples of Laughlin (A), Vu et al (B), van Hateren (C) and Grzywacz and Balboa (D). See text for details and complete references.

Table 1. *Comparison of parameters of contrast distributions for various studies and spatial sampling procedures*[a]

	−05C	−10C	−50C	Max	+50C	+10C	+05C
This Report 0.2	−80	−60	−16	−2.5	13	58	73
This Report 1.9	−50	−45	−10	−2.5	10	36	40
This Report 4.8	−48	−39	−15	+2.5	13	25	29
This Report 9.6	−55	−41	−17	−2.5	16	33	39
van Hateren 1.9	−32	−26	−12	−2.5	9	20	28
van Hateren 4.8	−53	−38	−7	+2.5	14	23	33
Laughlin 0.07/1.4	−56	−49	−28	−2.5	13	32	36
Vu 2	−63	−40	−17	−2.5	8	23	27
Balboa 1.9	−21	−17	−7	−2.5	6	16	19
Balboa 4.8	−31	−27	−8	+2.5	11	23	27

[a]The suffixes after the entries in the first column refer to the central reference area used to calculate contrast. The column headings refer to negative and positive contrast and the numbers, as in the body of the table, refer to the contrast magnitude in units of $\log_{10}$ contrast $\times 100$. In addition to the measurements of this report, the sources listed at the left are from the work of Laughlin, van Hateren, Vu et al., and Balboa and Grzywacz. See text for complete references for these sources.

tribution found in terrestrial natural images. Thus, these results for bipolar cells are in general agreement with the efficient coding hypothesis, first suggested by Laughlin (Laughlin, 1981, 1987) for interneurons in the invertebrate visual system.

We have performed additional experiments that show that, in the vertebrate retina, the correspondence with the natural image distribution is critically dependent on the joint action of light adaptation and signal transfer from cones to bipolar cells. Fig. 8A shows that the contrast/response function of cones (open circles) and horizontal cells (open squares) is much shallower than that of the depolarizing bipolar cells (filled circles) and the cumulative contrast distribution. It follows that mechanisms arising between the voltage response of cones and bipolar cells are critical for bringing the contrast response of bipolar cells into close registra-

tion with the contrast distribution in the natural environment. The results in Fig. 8A were obtained when the retina was light adapted to a background of 20 cd/m^2. The effect of reducing the level of light adaptation by attenuating the background field by a hundred-fold to 0.2 cd/m^2 is shown in Fig. 8B. The contrast/response curve of the bipolar cells (triangles) is now much shallower and thus not well matched to the image contrast distribution.

Distributed encoding in bipolar cells and the variance in natural image distributions

To this point, we have concentrated on the *average* contrast/response of bipolar cells. However, it has been shown that there is considerable variance in contrast/response curves within both the
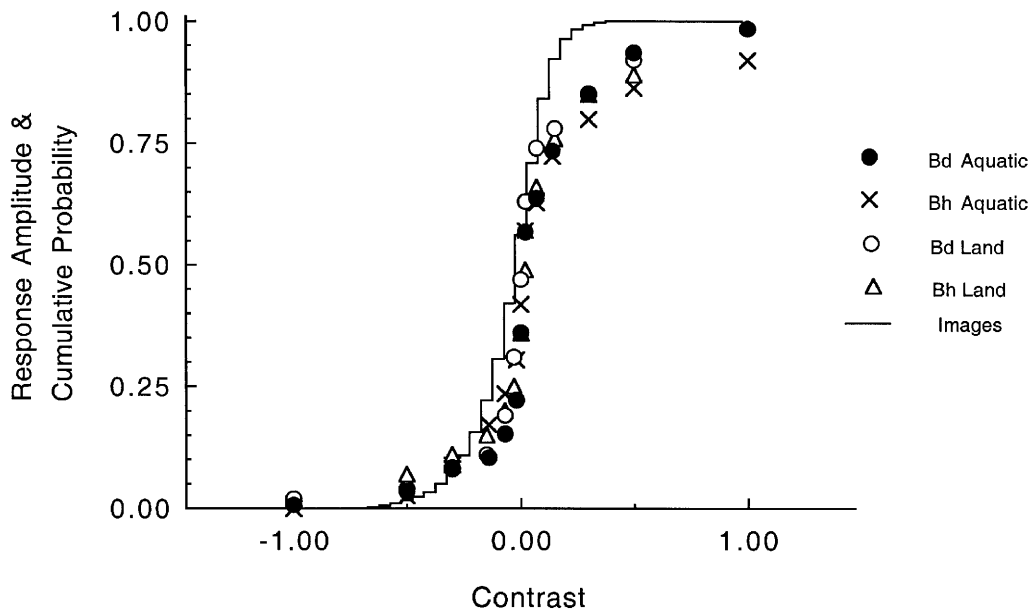
Fig. 7. Average contrast response curves for depolarizing (Bd) and hyperpolarizing (Bh) bipolar cells in aquatic- and land-phase animals. The solid line shows the cumulative probability for the average contrast distribution of the natural image sample of Fig. 5 (4.8-deg center). To facilitate comparisons, the curves for Bh cells are plotted so that positive contrasts evoke responses of positive polarity.
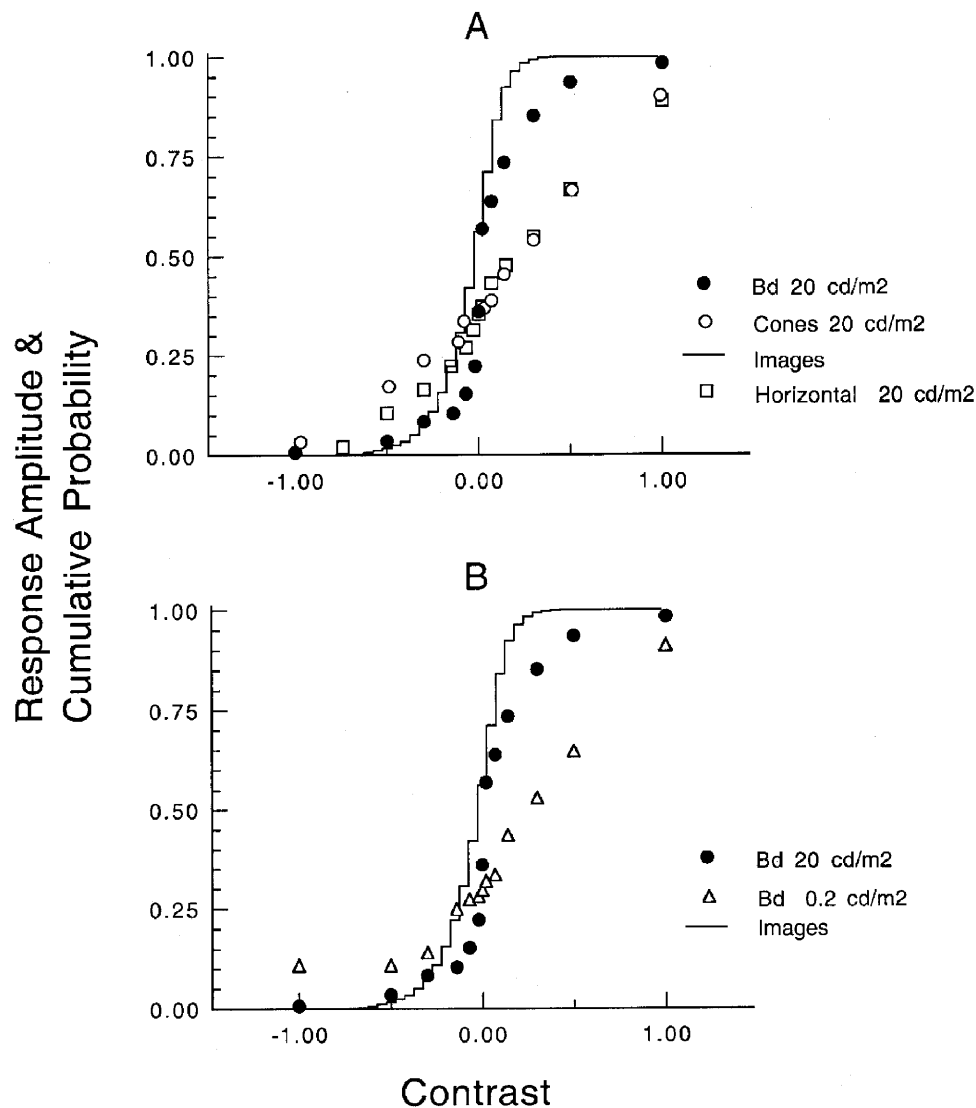
Fig. 8. A: Average contrast/response curves for cones and depolarizing bipolar cells of aquatic-phase animals under the standard light-adaptation conditions of 20 cd/m^2. The solid line is the same as in Fig. 7, showing the cumulative probability for the average contrast distribution of the natural image sample (Fig. 5, 4.8-deg center). Average curves for 63 Bd cells, 16 horizontal cells, and 8 cones. B: Average contrast/response curves for depolarizing bipolar cells of aquatic-phase animals under the standard light-adaptation conditions of 20 cd/m^2 (filled circles) and on a 100-fold weaker background of 0.02 cd/m^2 (open triangles).

Bh and Bd populations in aquatic animals (Burkhardt & Fahey, 1998; Fahey & Burkhardt, 2001). Fig. 9 shows that this is also the case for land-phase animals. Across both Bd (upper row) and Bh (lower row) populations, individual cells vary in contrast dominance. Thus, cells in column A are strongly negative-contrast dominant since they show a larger range of response to negative than to positive contrast, whereas cells in column C are strongly positive dominant. Cells in column B are more nearly balanced. For the cells in our sample, the range of distributed encoding in land-phase animals with respect to contrast dominance, contrast gain, and dynamic range was substantial and similar to that previously found for aquatic-based animals. As in aquatic animals, it was also found that differences in contrast gain were not highly correlated with measures of the contrast dominance based on half-maximal responses.

The dynamic range provides an index of the range of contrasts over which the bipolar cells might effectively respond to contrasts in the environment. Here, as in past work, we have quantified the dynamic range for each cell by determining the contrasts that give rise to responses that are 10% and 90% of the total response range. Due to differences in contrast dominance (Fig. 9), these values are often asymmetrical around zero contrast and thus extend much farther into either the positive or negative contrast domain, depending on the cell. In Fig. 10, we present measurements to evaluate the dynamic range of bipolar cells relative to the contrasts found in nature. The analysis for land animals (left panel) combines measurements from both Bh and Bd cells. The horizontal lines are drawn from the 10–90% contrast values and thus show the extent of the dynamic range for each cell in the sample. Cells have been ordered vertically in ascending order from those with the largest to smallest dynamic range. In all three panels, there are striking differences within the cell populations with respect to very narrow (top) or wide dynamic ranges (bottom) and asymmetry around the zero contrast. The large asymmetries reflect the exis-
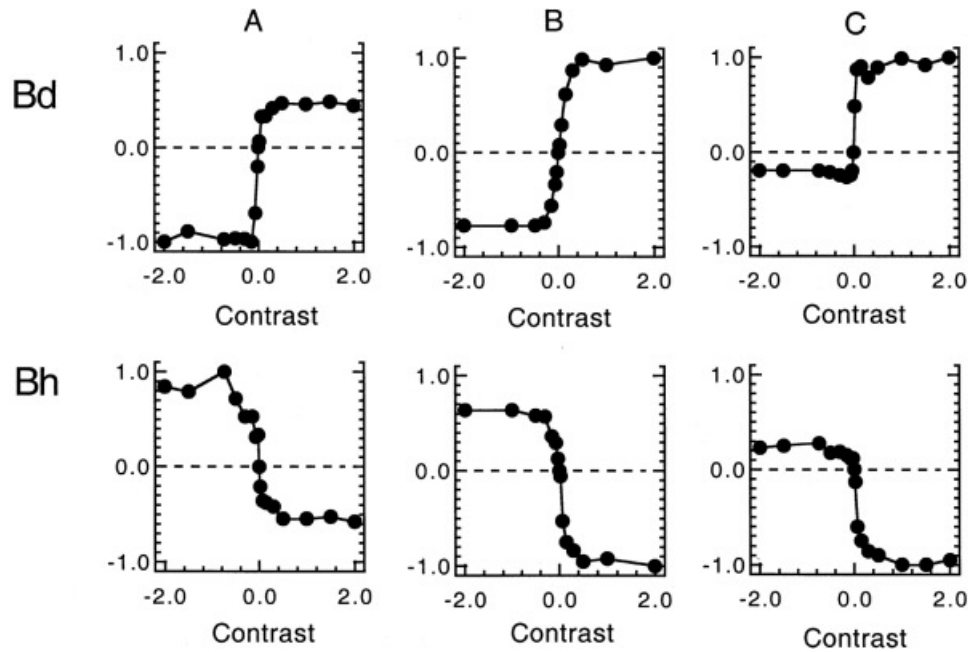
Fig. 9. Contrast/response curves for Bd cells (top row) and Bh cells (bottom row) on a background field of 20 cd/m² in land-phase animals. Spot diameter and total response range are: For Bd cells (A–C): 272 μm, 15 mV; 99 μm, 15.5 mV; 393 μm, 15.7 mV. For Bh cells (A–C): 272 μm, 12 mV; 99 μm, 15.2 mV; 272 μm, 20.4 mV.

tence of cells that show strong contrast dominance for either negative or positive contrast. The filled diamonds at the bottom of the graph show the average dynamic range of cones in aquatic-phase animals (Burkhardt & Fahey, 1998). The standard errors of these points are very small (not shown) and thus the diamonds can be taken as the fixed dynamic range of cones. Hence, Fig. 10 shows that the dynamic range of the vast majority of bipolar cells is considerably narrower, in some cases strikingly so, than that of cones. These differences further underscore the striking transformation in contrast encoding that takes place between the level of the cone photovoltage and the bipolar cell response.

The heavy lines in Fig. 10 show the average contrast histogram of our sample of 65 natural images, previously shown in Fig. 5 for the 4.8-deg reference. Thus, in all three panels, it is clear that the dynamic range of the bipolar cell population effectively brackets the range of contrasts found in nature. In a few cells, the dynamic range is very much narrower. On the other hand, in other cells, the range is substantially larger in one or both directions than that found in the sample of natural images. Among the three panels of Fig. 10, no striking differences are apparent for land versus aquatic animals or for Bh versus Bd cells. When analyzed *via* Student's *t* test, the mean
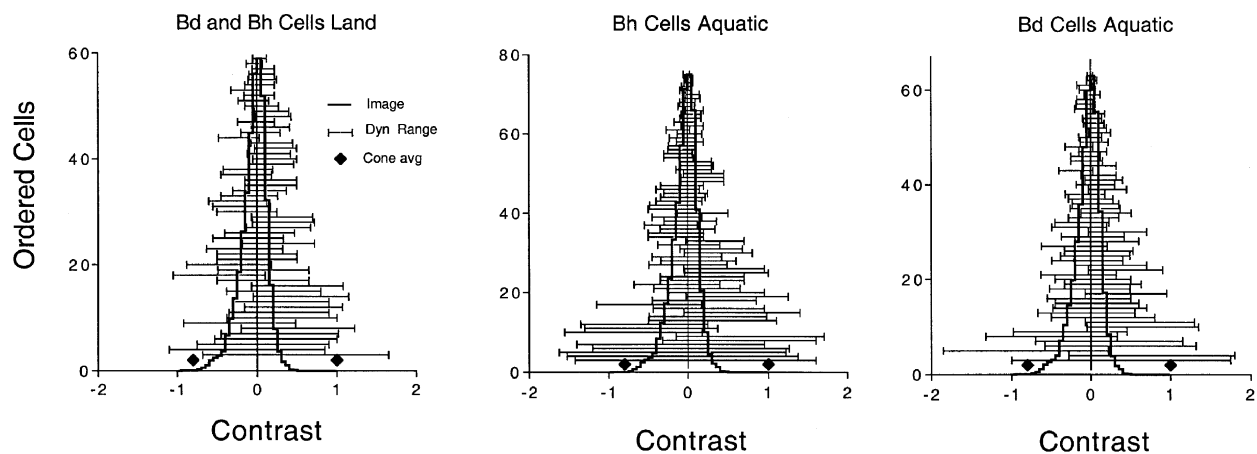
Fig. 10. Comparison of the distribution of dynamic ranges for contrast responses across the bipolar cell population and the natural image contrast distribution. The horizontal line shows the dynamic range encompassing 10–90% of the total response range for each cell. The heavy lines show the average natural image contrast distribution. A: Bd and Bh cells for land-phase animals. B and C, respectively: Bd and Bh cells for aquatic-phase animals. Diamonds show the dynamic range for cones of aquatic-phase animals.

values for the total dynamic range and the 10% and 90% points were not significantly different for land versus aquatic phase animals or for Bh versus Bd cells.

Discussion

Contrast distributions in natural images

Our measurements of natural images show that the average distributions are characterized by a vast preponderance of low contrasts. Thus, the distributions peak around zero contrast and then drop rapidly. Large contrasts were rare. This is all the more noteworthy since our sampling procedure was purposely biased toward high contrasts by emphasizing shadows, avoiding large uniform expanses of sky and water, and restricting measurements to conditions with strong sunlight (see Methods). Our spatial sampling procedure measured the contrast between a target area and a surrounding region eight times larger in area. The ratio and extent of the areas of the target and surrounding area were chosen to be comparable to that found experimentally for the receptive-field center and surround of bipolar cells (Fahey & Burkhardt, 2003). Increasing the diameter of the target area from 1.9 deg to 9.8 deg, and thereby spanning the approximate range of the receptive-field centers of the bipolar cell population, had only a modest broadening effect on the average distribution (Fig. 5). Thus, over this range, the average distribution was relatively independent of the sampling area, as suggested from some past observations (Laughlin, 1981; Ruderman & Bialek, 1994; Vu et al., 1997; Tadmor & Tolhurst, 2000). On the other hand, the distribution broadened appreciably (Table 1, top row) when the central reference square was made much smaller to subtend 0.2 deg, the approximate angular subtense of a salamander cone (equivalent to about 10 μm on the retina). The broadening seems expected on the grounds that the contribution of an extreme intensity in a very small target area will be given comparatively more weight when averages are computed over smaller areas.

Due to differences in spatial parameters, contrast metrics, and sites, it has been somewhat difficult to make quantitative comparisons across some previous reports on natural images. In this report, we have collected and transformed a body of data to provide a comparison of ten cases in a common format. The distributions were thereby shown to be in reasonably good quantitative agreement (Figs. 5 and 6 and Table 1). All tended to be narrow and somewhat skewed to the left. As might have been expected (Balboa & Grzywacz, 2003), the average contrast distributions for underwater images were somewhat narrower, and thus the range of contrasts even lower, than on land. On the other hand, the differences were relatively modest and our measurements provide an example of a terrestrial scene (Fig. 3B) whose contrast distribution (Fig. 4B) is narrower than that of the average underwater distribution (Fig. 6D). Moreover, the contrast distributions of terrestrial scenes will be even narrower when illumination is diffuse, as on cloudy days or under adverse weather conditions. Underwater distributions will also be narrowed by these factors but probably less so since even under the best conditions, light scatter is greater underwater than in air. Although our images were taken near ground level and avoided large expanses of sky or water, they were not obtained from the exact vantage of a small animal like the tiger salamander on land. However, since our distributions were already relatively narrow, it seems unlikely that the average distribution would be radically narrowed when taken from a vantage much closer to ground.

Contrast encoding in the outer retina

Fig. 7 shows that the average contrast/response curves of Bh and Bd cells, in both land-phase and aquatic-phase animals, are in reasonably close registration with the average distribution of contrasts in nature and thus in agreement within the efficient coding model of Laughlin (Laughlin, 1981, 1987). Computational modeling studies suggest efficient coding may also be found at the level of the ganglion cells in mammalian retinas (Tadmor & Tolhurst, 2000; Clatworthy et al., 2003). In support of Laughlin's hypothesis (Laughlin, 1987), the present results provide evidence that this encoding strategy is largely established distally, in the bipolar cells. The largest deviation from the contrast curve in Fig. 7 occurs for high positive contrasts. This discrepancy might be due to some bias in our image sample as discussed in Methods or it might be due to a true limitation of bipolar cells. Some amplification of the response for higher positive contrasts would then be needed centrally by higher visual neurons to achieve a better correspondence.

Our experiments of Fig. 8A show that nonlinear high-gain mechanisms between the cone photovoltage and the bipolar response are critical since the contrast/response curve of cones is much shallower than the cumulative contrast probability. This leads to the hypothesis that the nonlinear, high-gain transformation from cones to bipolar cells may have evolved because most contrasts in nature are, in fact, small (Figs. 4–6). There are a number of putative cellular mechanisms, which may play a role in this nonlinear, high-gain transformation (Thoreson & Burkhardt, 2003).

Since the contrasts of objects in nature are invariant with the intensity of the incident light, in the ideal case, efficient coding should hold over all ambient light intensities. However, in Fig. 8B we show that efficient coding in cone-driven bipolar cells is not achieved when the background light is low. Thus, light adaptation is critical for the emergence of efficient coding of contrast. This finding suggests a new and broader view of the function of light adaptation: When fully developed, light adaptation allows the retina to respond efficiently to the range of contrasts in the natural environment. From past work in vertebrate retinas, it is well established that light adaptation arises primarily at the level of the photoreceptors, but there is also evidence for additional mechanisms intrinsic to bipolar cells (Fahey & Burkhardt, 2001). The term "efficient coding," as used by Laughlin and in this report, means that the contrast response curve is in good agreement with the cumulative contrast distribution (Fig. 7). On this definition, the coding is not efficient at the lowest background intensity of 0.2 cd/m^2 (Fig. 8). It can be argued, however, that the coding might be viewed as efficient on a different criterion. Namely, if there were considerable noise in the photoreceptors at weak backgrounds, it might be efficient for the bipolar cells to have low gain and thus avoid generating large spurious signals. We think this unlikely, however, since our voltage recordings from salamander cones show relatively low noise (Burkhardt & Fahey, 1998; Fahey & Burkhardt, 2003).

Although Figs. 8A and 8B are based on recordings from aquatic-phase animals, these findings should also generalize to land-phase animals. We have analyzed recordings from horizontal cells in land-phase animals. The contrast/response curves, like that shown in Figs. 1B and 8A, were much shallower than that of bipolar cells (Fig. 7). It is highly likely that the contrast/response curve of cones will be no steeper, and probably shallower, than that shown in Figs. 1B and 8A. In land-phase animals, recordings were

held long enough to obtain contrast/response curves on 0.2 as well as on 20 cd/m^2 backgrounds for several bipolar cells. In agreement with the results in Fig. 8B, the contrast/response curves at 0.2 cd/m^2 were poorly matched with the cumulative contrast distribution.

It may be objected that our experiments and analysis, as in the reports of Laughlin (Laughlin, 1981, 1987), were restricted to responses to light flashes. In nature, flash-like events are rare and it is movement of objects in the environment that is the important stimulus for vision. With this in mind, we have investigated the response of bipolar cells to moving stimuli in detail in work to be published elsewhere. In any given cell, we found that the shape of the resulting contrast/response curves were very similar for flashes and movement when the moving stimuli were similar in dimensions to, and moved through, the center of the receptive field. If the trajectory of the moving stimuli or the position of flash stimuli was not optimum for stimulating the center of the receptive field, the responses were reduced but the shape of the curves was not greatly altered. Thus, it is likely that the general features of the results in the present report may be extended to the encoding of moving objects.

To adequately understand the basis of contrast encoding, the variance within the neuronal population is likely to be as important as the *average* response of the population. Largely due to technical difficulties of obtaining a large sample of intracellular recordings from bipolar cells, this issue will probably be very difficult, if not prohibitive, to pursue in most vertebrate retinas. The present report is therefore of special interest since we have been able to compare measurements across a sample of nearly 200 bipolar cells. In Fig. 10, we have summarized the distribution of the dynamic range found across the bipolar population. The width of the dynamic range, as shown by the horizontal lines, varies greatly from exceedingly narrow (cells at top) to quite broad. Equally striking and significant is the finding that the range is often asymmetric, and the direction of the asymmetry varies from cell to cell. Taken together, the measurements in Fig. 10 show that the distribution of the dynamic ranges of the bipolar cell population effectively brackets the distribution of contrasts found in natural images. This, in turn, suggests that the ability to encompass the effective range of contrasts in nature might have been the primary evolutionary force behind the establishment of distributed encoding in bipolar cells. Within the accuracy of our measurements, differences in dynamic range from cell to cell showed no consistent relation to the size of the receptive-field center.

Does the distribution of dynamic ranges in Fig. 10 represent optimum encoding? This seems unlikely since the dynamic range of some cells is quite broad and by definition, the calculated 10–90% dynamic range excludes 20% of the total response range. It is also known that the dynamic range broadens on weaker background intensities than the 20 cd/m^2 level of Fig. 10 (Fahey & Burkhardt, 2001). Perhaps there is some advantage to having some cells with very broad dynamic ranges or perhaps Fig. 10 represents the best that can be achieved within the constraints and variance of the biological machinery. There is evidence that the dynamic range may be narrowed somewhat further postsynaptically, in on–off amacrine and ganglion cells (Burkhardt & Fahey, 1999).

Contrast encoding in land-phase and aquatic-phase animals

For the purpose of the present research, it was necessary to obtain intracellular recordings from land-phase animals because our mea-

surements of natural images, as well as those of virtually all past work, were obtained in terrestrial environments. Despite the smaller size of retinal cells in land-phase animals, a reasonable sample of recordings (57 bipolar cells and 16 horizontal cells) was obtained. These recordings are of special interest since they are apparently the first to be reported for the land-phase tiger salamander. In marked contrast, the aquatic-phase tiger salamander has been studied extensively since the pioneering report of Werblin (Werblin, 1978) and has long served as an important animal model for the understanding of retinal function (for reviews, see Werblin, 1991; Wu, 1994, 2003).

When the aquatic-phase tiger salamander (also called larval, juvenile, or neotenous) matures later in life, it migrates from water to land and undergoes striking changes in physiology and morphology—shedding its external gills, developing a long slender tail, and decreasing in body size (Pough et al., 2001; Zug et al., 2001). Given these striking changes, we expected that the retinal organization might be substantially different in the land-phase animals. However, our measurements of contrast encoding in the outer retina of land-phase animals were quite similar to those for aquatic-phase animals. Thus, the extensive and diverse body of research on the aquatic-phase animal may, in large part, generalize to the mature, land-phase form. Although the anatomy of the retinas of land and aquatic retinas appeared relatively similar in observations of sections in paraffin-embedded material, the cell bodies of all classes of neurons where about 30% smaller in the land-phase animals. The smaller cell size probably explains why intracellular recordings were more difficult to obtain in land-phase animals.

With respect to the hypothesis that the transition to a terrestrial, aerial image-based visual environment might induce substantial changes in retinal organization, our results suggest the opposite. Thus, the neuronal mechanisms, first established in the aquatic phase, seem to be conserved and remain functionally stable. We suggest that this outcome, while perhaps surprising, may be understood within the context of a comparative analysis (Table 1) which indicates that the differences in contrast distributions on land and underwater may not be as great as supposed. Therefore, the contrast encoding mechanisms may be set in the aquatic-phase animal at a level that is reasonably efficient to accommodate subsequent life on land, thereby circumventing the need for extensive reorganization of the retina.

Acknowledgments

References

Balboa, R.M. & Grzywacz, N.M. (2003). Power spectra and distribution of contrasts of natural images from different habitats. *Vision Research* **43**, 2527–2537.

Burkhardt, D.A. (2001). Light adaptation and contrast in the outer retina. In *Progress in Brain Research. Concepts and Challenges in Retinal Biology. A Tribute to John E. Dowling, Vol. 131*, ed. Kolb, H., Wu, S. & Ripps, H., pp. 407–418. Amsterdam: Elsevier.

Burkhardt, D.A. & Fahey, P.K. (1998). Contrast enhancement and distributed encoding by bipolar cells in the retina. *Journal of Neurophysiology* **80**, 1070–1081.

BURKHARDT, D.A., FAHEY, P.K. & SIKORA, M. (1998). Responses of ganglion cells to contrast steps in the light-adapted retina of the tiger salamander. *Visual Neuroscience* **15**, 219–229.

BURKHARDT, D.A. & FAHEY, P.K. (1999). Contrast rectification and distributed encoding by on-off amacrine cells in the retina. *Journal of Neurophysiology* **81**, 1676–1688.

BURKHARDT, D.A., FAHEY, P.K. & SIKORA, M.A. (2004). Retinal bipolar cells: Contrast encoding for sinusoidal modulation and steps of luminance contrast. *Visual Neuroscience* **21**, 883–893.

CLATWORTHY, P.L., CHIRIMUUTA, M., LAURITZEN, J.S. & TOLHURST, D.J. (2003). Coding of contrasts in natural images by populations of neurones in primary visual cortex (V1). *Vision Research* **43**, 1983–2001.

COPENHAGEN, D.R. (2004). Excitation in the retina: The flow, filtering, and molecules of visual signaling in the glutamatergic pathways from photoreceptors to ganglion cells. In *The Visual Neurosciences, Vol. 1*, ed. CHALUPA, L.M. & WERNER, J.S., pp. 320–333. Cambridge, Massachusetts: MIT Press.

DACEY, D., PACKER, O.S., DILLER, L., BRAINARD, D., PETERSON, B. & LEE, B. (2000). Center surround receptive field structure of cone bipolar cells in primate retina. *Vision Research* **40**, 1801–1811.

DEVRIES, S.H. (2000). Bipolar cells use kainate and AMPA receptors to filter visual information. *Neuron* **28**, 847–856.

FAHEY, P.K. & BURKHARDT, D.A. (2001). Effects of light adaptation on contrast processing in bipolar cells in the retina. *Visual Neuroscience* **18**, 581–597.

FAHEY, P.K. & BURKHARDT, D.A. (2003). Center-surround organization in bipolar cells: Symmetry for opposing contrasts. *Visual Neuroscience* **20**, 1–10.

HARE, W.A. & OWEN, W.G. (1990). Spatial organization of the bipolar cell's receptive field in the retina of the tiger salamander. *Journal of Physiology* (London) **421**, 223–245.

HARE, W.A. & OWEN, W.G. (1995). Similar effects of carbachol and dopamine on neurons in the distal retina of the tiger salamander. *Visual Neuroscience* **12**, 443–455.

LAUGHLIN, S.B. (1981). A simple coding procedure enhances a neuron's information capacity. *Zeitschrift Naturforschung* **36c**, 910–912.

LAUGHLIN, S.B. (1987). Form and function in retinal processing. *Trends in Neuroscience* **10**, 478–483.

NELSON, R. & KOLB, H. (2004). ON and OFF pathways in the vertebrate retina and visual system. In *The Visual Neurosciences, Vol. 1*, ed. CHALUPA, L.M. & WERNER, J.S., pp. 260–278. Cambridge, Massachusetts: MIT Press.

POUGH, F.H., ANDREWS, R.M., CADLE, J.E., CRUMP, M.L., SASVITZKY, A.H. & WELLS, K.D. (2001). *Herpetology*. Upper Saddle River, New Jersey: Prentice Hall.

RIEKE, F. (2001). Temporal contrast adaptation in salamander bipolar cells. *Journal of Neuroscience* **21**, 9445–9454.

RUDERMAN, D.L. & BIALEK, W. (1994). Statistics of natural images: scaling in the woods. *Physical Review Letters* **73**, 814–817.

SIMONCELLI, E.P. & OLSHAUSEN, B.A. (2001). Natural image statistics and neural representation. *Annual Review of Neuroscience* **24**, 1193–1216.

STERLING, P. (2004). How retinal circuits optimize the transfer of visual information. In *The Visual Neurosciences, Vol. 1*, ed. CHALUPA, L.M. & WERNER, J.S., pp. 234–259. Cambridge, Massachusetts: MIT Press.

TADMOR, Y. & TOLHURST, D.J. (2000). Calculating the contrasts that retinal ganglion cells and LGN neurones encounter in natural scenes. *Vision Research* **40**, 3145–3157.

THORESON, W.B. & BURKHARDT, D.A. (2003). Contrast encoding in retinal bipolar cells: Current vs. voltage. *Visual Neuroscience* **20**, 19–28.

VU, T.Q., MCCARTHY, S.T. & OWEN, W.G. (1997). Linear transduction of natural stimuli by dark-adapted and light-adapted rods of the salamander, *Ambystoma tigrinum*. *Journal of Physiology* **505**, 193–204.

WERBLIN, F.S. (1978). Transmission along and between rods in the tiger salamander retina. *Journal of Physiology* **280**, 449–470.

WERBLIN, F.S. (1991). Synaptic connections, receptive fields, and patterns of activity in the tiger salamander retina. *Investigative Ophthalmology* **32**, 459–483.

WERBLIN, F.S. & DOWLING, J.E. (1968). Organization of the retina of the mudpuppy, Necturus maculosus. II. Intracellular recording. *Journal of Neurophysiology* **32**, 339–355.

WU, S.M. (1994). Synaptic transmission in the outer retina. *Annual Review of Physiology* **56**, 141–168.

WU, S.M. (2003). Intracelluar light responses and synaptic organization of the vertebrate retina. In *Adler's Physiology of the Eye*, 10th edition, ed. KAUFMAN, P.K. & ALM, A., pp. 422–438. St. Louis, Missouri: Mosby.

YANG, X.L. & WU, S.M. (1991). Feedforward lateral inhibition in retinal bipolar cells: Input–output relation of the horizontal cell-depolarizing bipolar cell synapse. *Proceedings of the National Academy of Sciences of the U. S. A.* **88**, 3310–3313.

ZUG, G.R., VITT, L. & CALDWELL, J.P. (2001). *Herpetology*, 2nd ed. San Diego, California: Academic Press.